Topology optimization of a U-bend tool using LS-TaSC

David Aspenberg[1], Nader Asnafi[2]

[1]DYNAmore Nordic AB, Linköping, Sweden
[2]Örebro University, School of Science & Technology, Örebro, Sweden

1 Abstract

Metal additive manufacturing of stamping tool and die has a potential of reducing the lead time of forming processes, while at least not increasing the cost. As a part of a research project exploring the possibilities to use this type of tool manufacturing techniques, topology optimization using LS-TaSC has been utilized and one example case is presented in this paper, namely a U-bend tool. This paper looks at the possible benefits from using nonlinear simulations in topology optimization, the effect of chosen target mass fraction value, the interpretations needed of optimal results and the effects on the formed specimen after using an optimized tool. Results show that accounting for the time dependent pressure on the tool, rather than applying a form of equivalent static load, gives a different optimal topology. Some manual interpretations of the optimal results are also recommended, as well as studying the effects on the specimen from removing material on the tool side.

2 Introduction

Digi3D is the name of a national research program in Sweden, partly funded by the Swedish government agency Vinnova, but also with several industrial and academic partners. [1] The project states that: “The lead time for the production of tools and dies for a new car body is currently about 12 months and needs to be reduced 40% by 2020.” For this reason, one of the subprojects in the Digi3D research program investigated how metal additive manufacturing (henceforth also called 3D printing or AM) based on Laser-based Powder Bed Fusion (LPBF) could influence the lead time for, as well as the costs of, stamping tool & die design and manufacturing. DYNAmore Nordic, as one of the industrial partners in Digi3D, has contributed by performing topology optimization studies on selected industrial tools.

In this paper, the focus is put on the application of LS-TaSC on a U-bend tool. While applying topology optimization on this tool, we have tested many different things in order to build confidence for the topology optimization and study the effect of different choices in the problem setup, and would therefore like to discuss the following questions:

- What are the benefits, if any, of performing the topology optimization directly on the full nonlinear process simulation?
- How does the selection of the target mass fraction value affect the solution?
- What level of interpretation is required when going from the optimal solution to a design suggestion?
- For a forming simulation, is the test specimen affected when material is removed from the tool which makes the tool more compliant?

In addition to the numerical results, some of the experimental results from using the topology optimized 3D printed U-bend tool are presented.

3 Topology optimization

Most topology optimization methods use sensitivity information to drive the search for an optimum, as the sensitivity calculus is computationally relatively inexpensive for linear problems. Nonlinear topology optimization problems with high computational function evaluations on the other hand require alternative methods.

The methodology in LS-TaSC is suitable for dynamic problems and is always evolving. It is therefore best referred to as simply the LS-TaSC method, accompanied by version number. [2] The development of LS-TaSC is driven by

- the lack of gradient information for crashworthiness problems (more precisely nonlinear problems in general)
- the very large problems being considered in practice
- the integration of topology optimization into the overall design process

More details regarding the LS-TaSC methodology is best covered in the theory manual of the software [3], but also some past conference papers are good for orientation purposes, such as [4]-[6].

The focus of this study has not been on applying different parameter settings in LS-TaSC to tweak the results, but rather to use default settings. This keeps things simple and eliminates possible setup differences between optimization runs. However, as one of the consequences, some optimizations have stopped based on the minimum mass redistribution criterion, even though the topology has not yet reached a 0/1 state. The maximum number of iterations criterion on the other hand has been set so high that it has not been reached.

4 FE model

A symmetry model of the U-bend operation has been used, where the red part in Figure 1 constitutes the design domain. The specimen that is bent is of DP600 steel material, 2 mm thick and is modelled with **`MAT_133`** (Barlat, YLD200), whereas the grey parts are rigid and the transparent part and the red part are elastic.

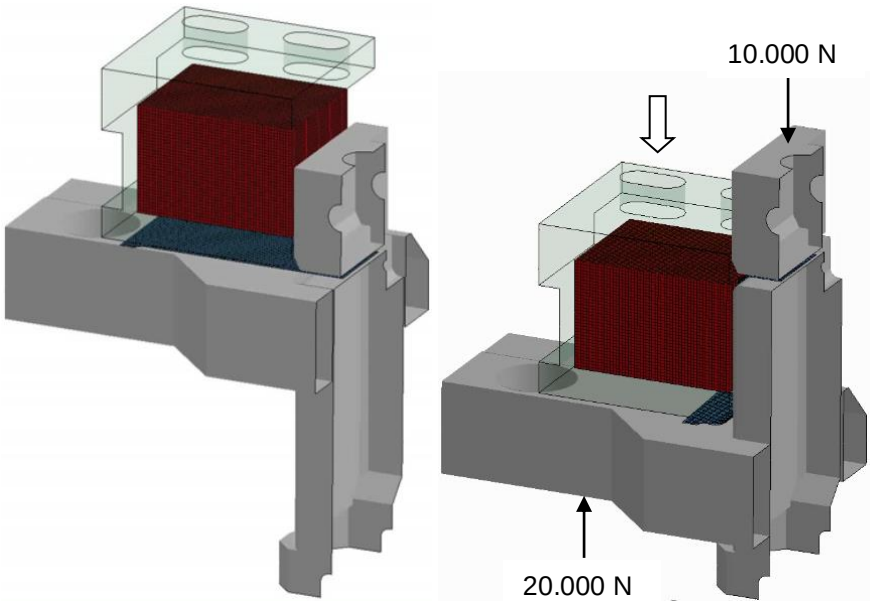

Fig.1: FE model for the U-bend simulation, symmetry model.

The test specimen is first clamped between the tools with forces according to Figure 1. These forces are constant through the simulation. Then, a prescribed vertical displacement of the upper surface of the transparent part is applied, a surface which is only free to move in the vertical direction. **`*CONTACT_FORMING_SURFACE_TO_SURFACE`** is used with static and dynamic friction set to 0.125, except for the contact between part subjected to 10.000 N and the specimen where the friction is set to 0.35, to compensate for the tool surface in reality being knurled, and not planar as in the model. Mass scaling is applied, adding 1.7 % of mass to the model.

5 Optimization results

The work in this project started with 2D simulations of the tool. In Figure 2 the models along with the optimal solutions are presented. The top surfaces of these models are constrained in both directions and the model is loaded with pressure loads according to the figure.

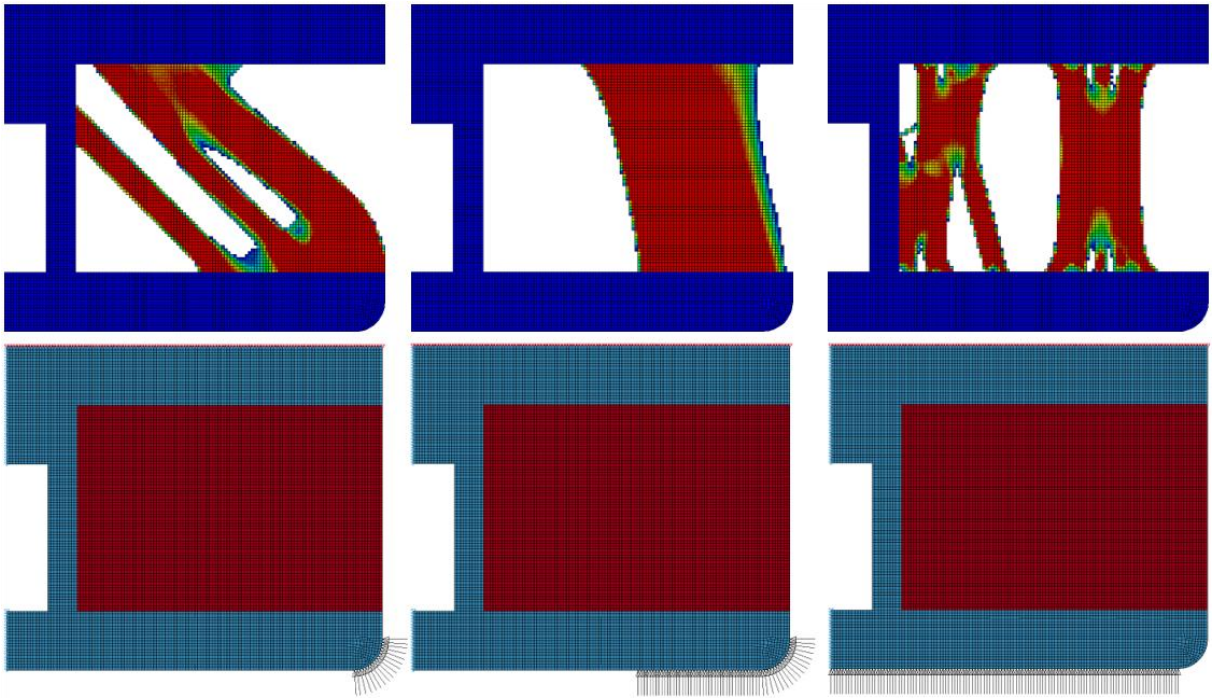

Fig.2: Optimal 2D solutions given different constant static loads.

The trivial result from Figure 2 is of course that the distribution of the load (and the boundary conditions) completely determines the optimal configuration of the design domain. These simple optimizations were followed by attempts to better estimate the loads that should be applied. From the simulation of the full 3D process, the pressures on the tools were recorded through the keyword **`*DATABASE_BINARY_INTFOR`**. The pressures were then summed over the width of the specimen and applied to the 2D model of the tool in three different ways: a) using only the maximum pressure value recorded, b) using an integrated value over time of the pressure in the simulation or c) as time dependent pressures, cf. Figure 3.

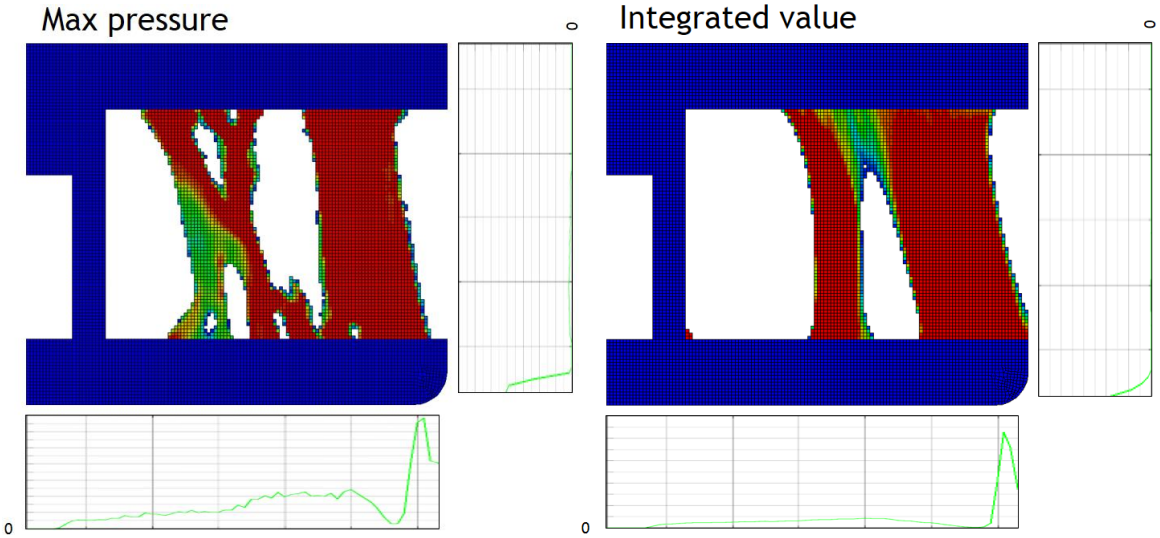

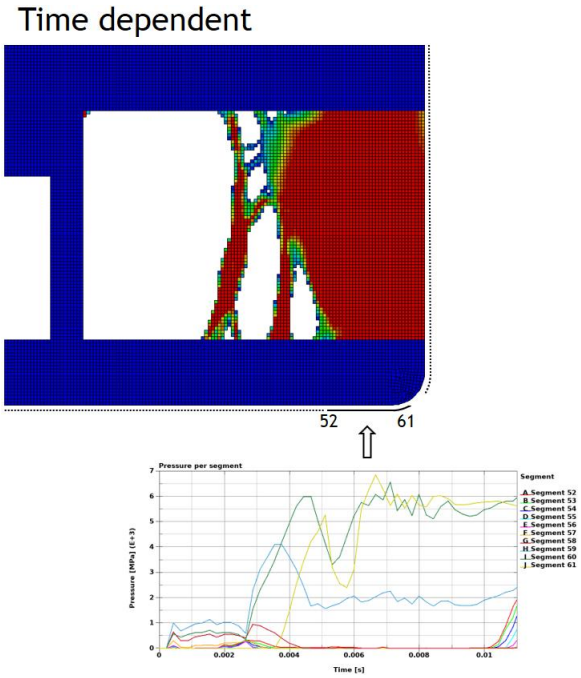

Fig.3: Optimal 2D solutions given loads from the 3D simulation of the process. The load is applied along the entire bottom and right boundaries. In the top left, the maximum pressure value recorded is applied, in the top right an integrated value over time of the recorded pressure is applied and in the bottom a time dependent pressure value is applied which also varies along the boundary.

The same tool has also been optimized in another topology optimization software called TopoBox, see Figure 4 and [7]. However, the settings that were used in this optimization, e.g. in terms of loads or boundary conditions, or even the techniques applied, is not known to the authors. A similar topology inspired by this solution is included here only for comparison purposes, since it also presents a plausible solution to the problem.

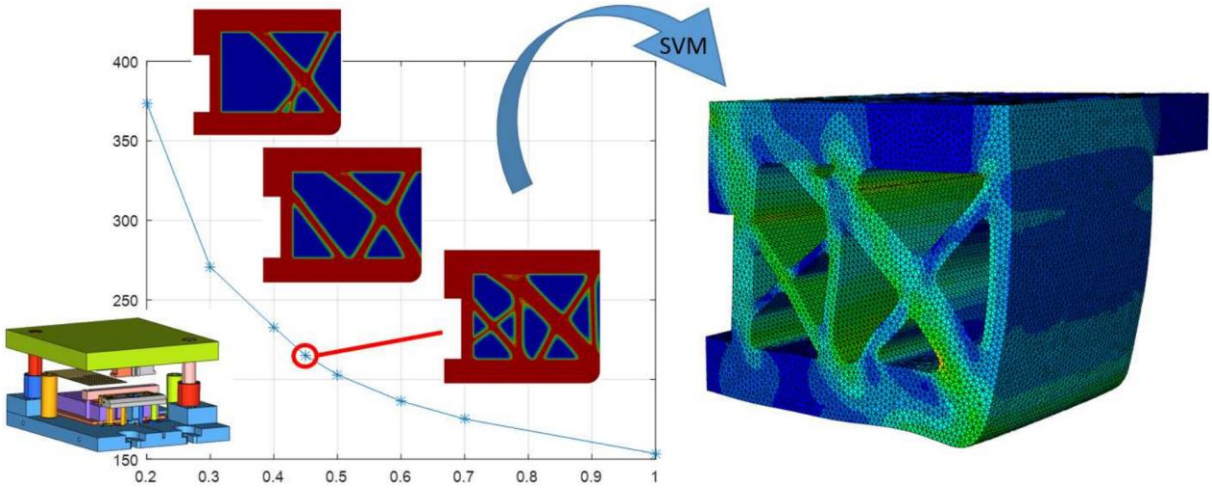

Fig.4: Optimal solution of the same tool using TopoBox, image from [7].

Finally, the full 3D model was used directly for topology optimization. To be able to make comparisons between the other suggested solutions, it was decided to add an extrusion constraint in the width direction, i.e. the cross section of the tool is unchanged over the width. The optimal solutions from using the full 3D model of the process and optimization with LS-TaSC can be seen in Figure 5.

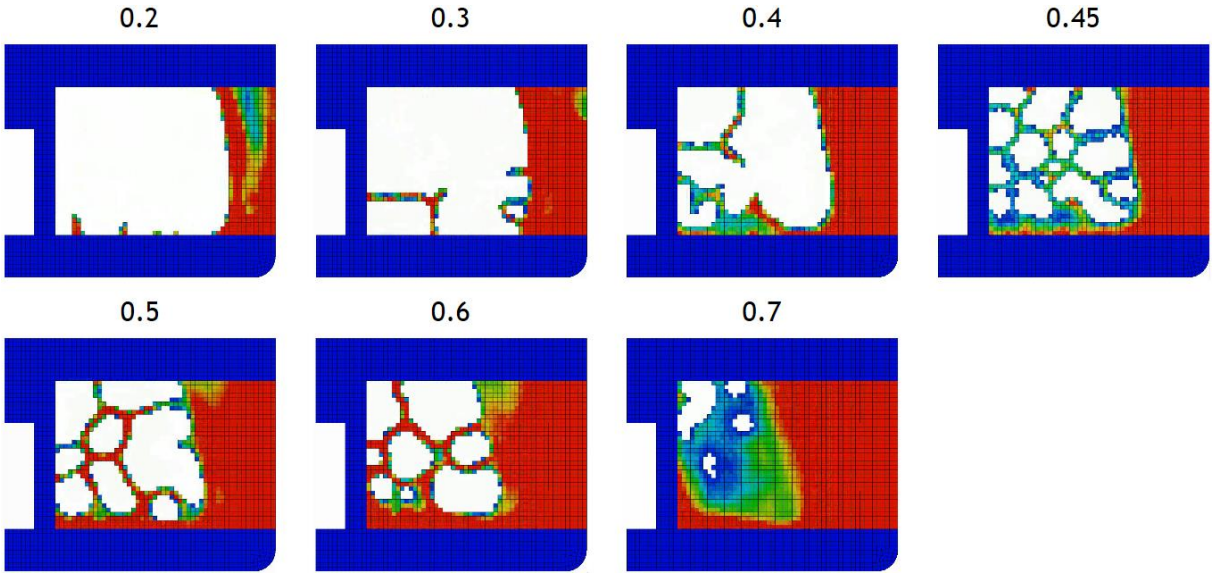

Fig.5: Optimal solutions when using different target mass fractions. The fringe scale shows the mass fraction (the design region only), where a value between near zero (almost no material) is blue and a value near one (filled with material) is red. White color means that the elements contain no material and has been removed from the model.

6 Evaulations of selected optima

Four different suggestions for optimal solutions have been selected and evaluated, along with the original solid tool. The four selected optimal solutions are presented in Figure 6.

Fig.6: Selected optimal topologies. These are given the names from the left LS-TaSC 0.3, Topobox, LS-TaSC 0.45 and Hole lattice.

Model	Design area (mm²)	Max. von Mises stress (MPa)
LS-TaSC 0.3, interpreted	526 (28.9%)	135
Topobox	882 (48.5%)	407[1] (250)
LS-TaSC 0.45	1142 (62.8%)	205
Hole lattice	1316 (72.3%)	158
Solid tool	1820	128

Table 1: Comparison between evaluated suggested optima sorted by ascending mass fraction values.

[1] This values comes from a corner stress concentration at the end of the simulation. A more realistic value without this effect is around 250 MPa, cf. Figure 7.

Three measures have been used to evaluate the tools, the mass fraction of the design region, the maximum von Mises stress in the design region during the complete simulation and the vertical displacement time history of a node slightly above the draw radius. Additionally, the thickness reduction of the specimen has been evaluated as a measure of how stretched they have been during the forming.

The first two measures are presented in Table 1: above and in Figure 7. It should be noted that even though the target mass fraction in the two evaluated LS-TaSC solutions were set to 0.3 and 0.45, the realization of these suggested optima slightly altered the mass fraction.

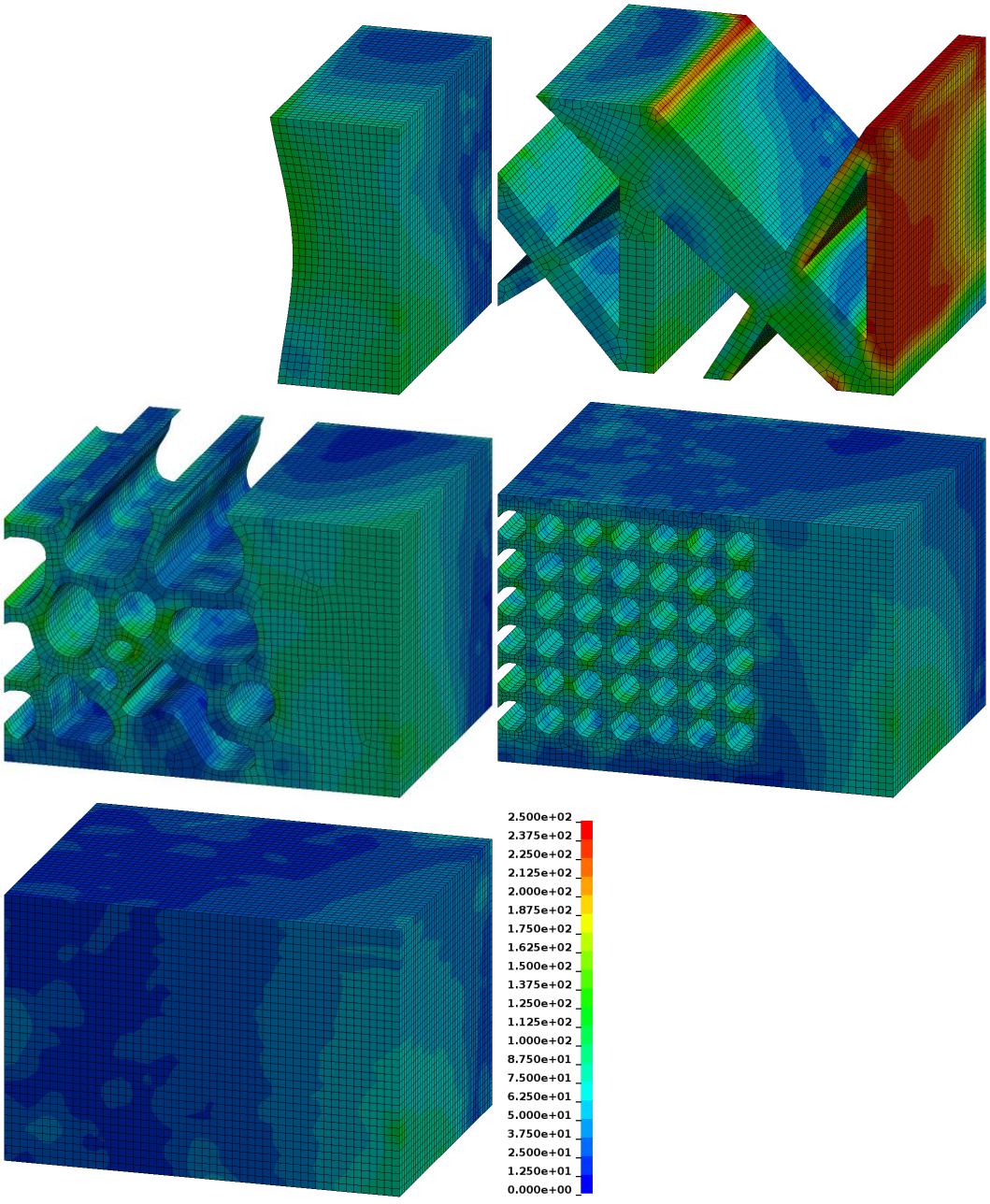

Fig.7: Fringe plot of the maximum von Mises stresses during the whole forming process for the four suggested optima and a solid design volume.

The stiffness evaluation at the draw radius for the optima presented in Figure 5 is presented in Figure 8, whereas the results for the suggested optimal solutions are presented in Figure 9.

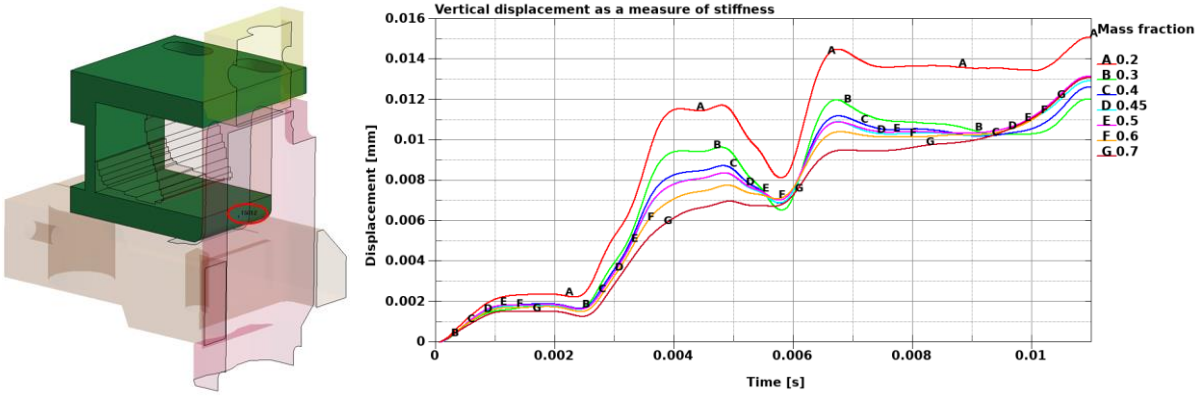

Fig.8: Vertical displacement of a selected node on the optimized tool. The results for the optimal solutions in Figure 5 are presented.

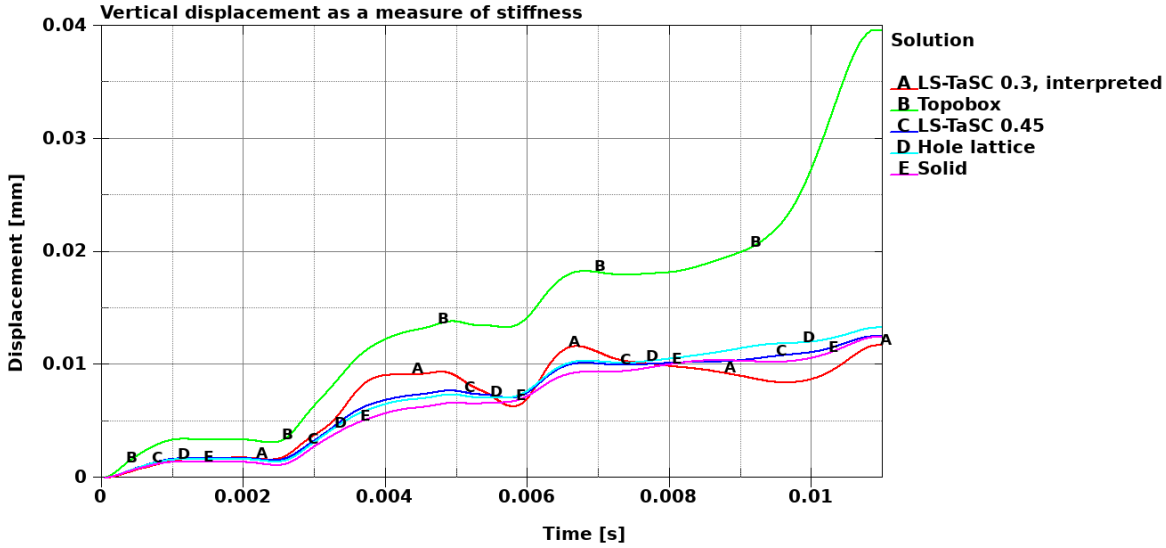

Fig.9: Vertical displacement of a selected node on the optimized tool, the results for the selected optimal solutions.

Finally, the thickness reduction of the specimen has been evaluated. Again, the results for the optimal solutions in Figure 5 are presented in Figure 10, whereas the results for the suggested optima are presented in Figure 11. Additionally, some special cases were evaluated in order to investigate the changes that comes from moving from rigid tools to an elastic tool. The impact on the specimens from these simulations are presented in Figure 12.

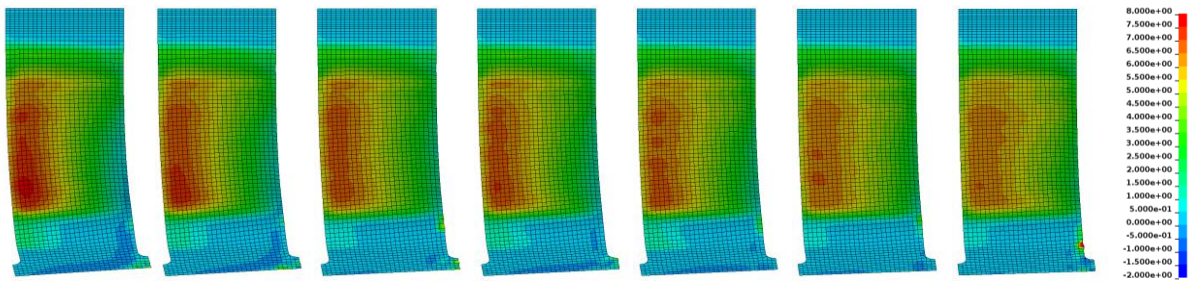

Fig.10: Percental thickness reduction on specimen when using increased mass fraction. The mass fractions are from the left: 0.2, 0.3, 0.4, 0.45, 0.5, 0.6 and 0.7.

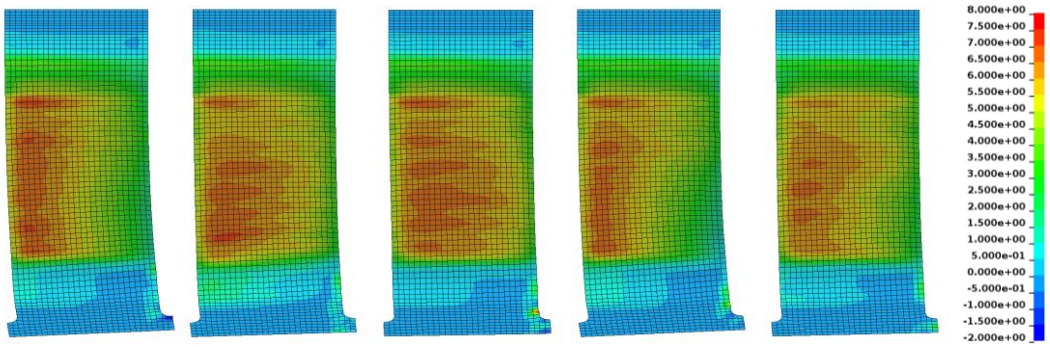

Fig.11: Percental thickness reduction on specimen. The models are from the left: LS-TaSC 0.3, Topobox, LS-TaSC 0.45, Hole lattice and Solid tool.

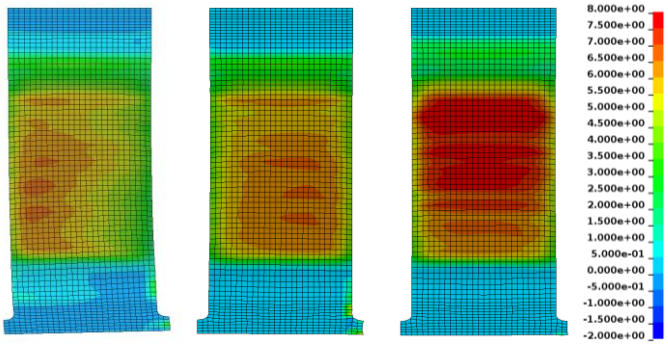

Fig.12: Percental thickness reduction on specimen effect of elastic tools. The models are from the left: elastic tool rigid blankholder, all tools rigid and elastic tools elastic blankholder.

7 Experimental results

To fully test the concept of 3D printed optimized tools, the topology optimized tool, named LS-TaSC 0.45, was 3D printed in the maraging steel[2] DIN 1.2709. For comparison purposes, a solid design version of the tool was also printed, cf. Figure 13. The topology optimized version reduced the tool weight (or improved the material usage) by 19.4% and reduced the production lead time by 11.1% compared to the solid version of the tool.

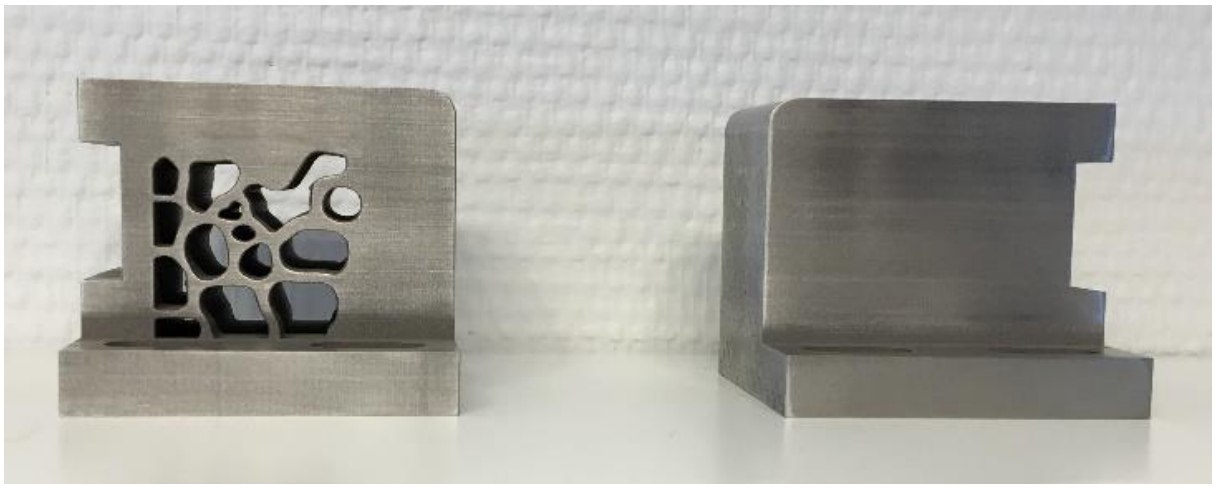

Fig.13: 3D printed U-bend tools, topology optimized version to the left and solid tool to the right.

[2] The word maraging is a portmanteau (blend) of “martensitic” and “aging”. The characteristics of this type of steel is the possession of superior strength and toughness without losing ductility.

Both tool halves were subjected to 50,000 strokes forming DP600 material of 2 mm thickness. Initially, the profile radius of the topology optimized tool half was 5.05 mm and that of the solid tool half was 5.04 mm. After 50,000 strokes, the maximum wear measured as a change in the profile radius was only 0.0186 mm. Figure 14 shows a comparison of the surface scratches on the specimen on using the two printed versions of the tool. An equal binder force on both sides has been applied, but there are still less scratches on the topology optimized version of the tool, which is yet to be explained.

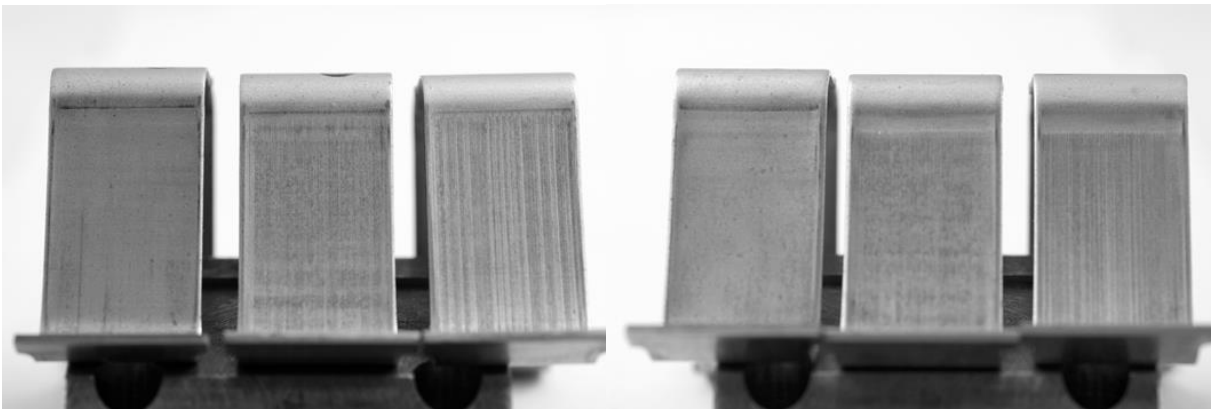

Fig.14: Image of surface scratches on the specimens from the first stroke, 25 thousand strokes and 50 thousand strokes, respectively. The specimens on the left side are from the solid 3D printed tool and on the right side from the topology optimized and 3D printed tool.

A separate evaluation of the springback would perhaps also be interesting, but this has not been performed at this time. More details on the experimental study can be found in [8] and [9].

8 Discussion

Looking at the results from the optimal solution denoted LS-TaSC 0.3, it seems that 70% of the material in the design volume could easily be removed. The maximum von Mises stress during the forming process is not much higher than in the solid tool and the stiffness of the tool in terms of movements during the forming is not much larger either. The material may however not be placed arbitrarily in the design volume, which is demonstrated by the large difference between the different proposed optima. Most material should be placed above the draw radius, which is also the region where the largest pressures on the tool are recorded.

The effect of raising the mass fraction gives satisfying results in terms of material not being redistributed to other regions as the amount of material increases, which seems intuitively right. The effect of applying constant loads in 2D instead of simulating the full process in 3D is much larger. If one assumes that a 2D model would give approximately the same results as a 3D model with an extrusion constraint, it does seem important to at least use time-varying loads to get a similar optimal topology.

One of the most positive things about this study was how easy it was to go from the process simulation to the topology optimization. To get an LS-TaSC model, it was enough to define a separate part in the LS-DYNA model that could constitute the design volume. Then a mass fraction value, an extrusion constraint and an execution command for the solver was set in LS-TaSC. Translating loads from the process simulation to a linear model, possibly also working with two different solvers, is a process that most likely would be more costly. The downside of using the full process simulation directly is when this simulation is a computationally costly operation, since a model evaluation is performed in each iteration.

One difference in results that has not been investigated further in this study is the increase in thickness reduction of the specimen when using less material in the tool. This would be an interesting investigation in itself, since a large difference in results can be seen when simply changing from rigid to elastic tools in the simulation, even though the forming process with all its parameters is kept constant.

9 Summary

Topology optimization of a forming tool has been performed using the full process simulation directly. One major benefit from this approach is the easy setup moving from an existing simulation model of the forming process to a topology optimization. The optimal solutions retrieved are not the same when using simplified load applications. It seems relevant to use the actual process simulation without simplifications. The possible downside of this approach might be an increase in computational cost since the process simulation itself might be computationally expensive. It is furthermore recommended that some engineering judgement of the suggested optimal topology is performed in order to make some possible simplifications to the final design. Finally, some effects on the formed specimen is also noted depending on the amount of material removed from the tool, but this needs to be investigated further. The large difference on the specimen results is observed when moving from rigid to elastic tools.

10 Acknowledgements

The authors would like to thank Sweden's Innovation Agency Vinnova for funding this investigation and 3D MetPrint, Dynamore Nordic, Hydroforming Design Light, IKEA, Ionbond Sweden, Melament, Nolato Lövepac, PLM Group, RISE IVF, Volvo Cars, Uddeholm and Örebro University for a fruitful and efficient collaboration.

11 Literature

[1] https://www.digi3d.org/, visited 2019-02-01.
[2] Livermore Software Technology Corporation, The LS-TaSC™ Tool Topology and Shape Computations – User's manual, Version 3.2, 2016.
[3] Livermore Software Technology Corporation, The LS-TaSC™ Tool – Theory manual, Version 3.2, 2016.
[4] Roux, W.: "The LS-TaSC™ multipoint method for constrained topology optimization", 14th International LS-DYNA Users Conference, June 12–14, 2016, Detroit.
[5] Witowski, K., Roux, W.: "LS-TaSC™ product status", 11th European LS-DYNA conference, 2017, Salzburg, Austria.
[6] Roux, W., Yi, G., Gandikota, I.: "Implementation of the projected subgradient method in LS-TaSC™", 15th International LS-DYNA® Users Conference, June 10–12, 2018, Detroit.
[7] Strömberg, N: "Automatic postprocessing of topology optimization solutions by using support vector machines", Proceedings of the ASME 2018 International Design Engineering Technical Conferences & Computers and Information in Engineering Conference IDETC/CIE, August 26–29, 2018, Quebec City, Canada.
[8] Asnafi, N., Shams, T., Aspenberg, D., Öberg, C., "3D Metal Printing from an Industrial Perspective — Product Design, Production, and Business Models", Berg Huettenmaenn Monatsh, Vol. 164 (3): 2019, 91–100. (Beiträge der Metal Additive Manufacturing Conference 2018)
[9] Asnafi, N., Rajalampi, J., Aspenberg, D., "Design and Validation of 3D Printed Tools for Stamping of DP600", International Deep Drawing Research Group Conference, June 3–7, 2019, Enschede, Netherlands.